BULLETIN OF THE POLISH ACADEMY OF SCIENCES
TECHNICAL SCIENCES, Vol. 72(4), 2024, Article number: e150111
DOI: 10.24425/bpasts.2024.150111

Comprehensive online estimation of object signals for a control system with an adaptive approach and incomplete measurements

Tadeusz KWATER[1]*, **Przemysław HAWRO**[1], **Paweł KRUTYS**[1], **Marek GOŁĘBIOWSKI**[2], and **Grzegorz DRAŁUS**[2]

[1] Faculty of Technical Engineering, State University of Applied Sciences in Jaroslaw, Poland
[2] Faculty of Electrical and Computer Engineering, Rzeszow University of Technology, Poland

Abstract. This paper presents the novel estimation algorithm that generates all signals of an object described by nonlinear ordinary differential equations based only on easy-to-implement measurements. Unmeasured signals are estimated by using an adaptive approach. For this purpose, a filtering equation with a continuously modified gain vector is used. Its value is determined by an incremental method, and the amount of correction depends on the current difference between the generated signal and its measured counterpart. In addition, the study takes into account the aging process of measurements and their random absence. The application of the proposed approach can be realized for any objects with a suitable mathematical description. A biochemically polluted river with an appropriate transformation of the notation of partial differential equations was chosen as an object. The results of numerical experiments are promising, and the process of obtaining them involves little computational necessity, so the approach is aimed at the needs of control implemented online.

Keywords: online estimation and control; nonlinear differential equations; adaptive gain modification; measurements window; random lack of measurements.

1. INTRODUCTION

Rivers are crucial to the global hydrological cycle, ecosystems, and human economy and life. Therefore, river water quality is of great concern. River water quality is constantly deteriorating, and the main reason for water pollution is mainly due to human activities. Every year, millions of tons of waste, industrial, agricultural and municipal wastewater, are discharged into rivers, making the water unusable and requiring frequent quality control. In addition to human impacts, the state of water in rivers is also affected by weather conditions, necessitating continuous monitoring with control and management functions for water management in the region [1–5]. Traditional methods of assessing water quality involve taking samples and testing them in a laboratory, which is time-consuming as a result of which information on the state of water quality is usually overdone. Real-time systems that take measurements easily online and reproduce unmeasured signals may be the answer to these challenges. The authors in [6, 7] suggest the use of mobile measuring stations and mobile operating systems for real-time monitoring of various water parameters in rivers. In [8] the authors propose an adaptive sampling algorithm to increase energy efficiency in automatic monitoring systems while ensuring the accuracy of the sampled data. Tests conducted in this study included measurement of dissolved oxygen (DO) and water turbidity. Real-time water quality monitoring systems using chemical sensors have been discussed in [9–11]. The authors emphasize that systems based on chemical detection or a combination of chemical and other methods are the most effective. However, many real-time monitoring systems do not offer the ability to measure all required signals online. In the case of rivers, one such signal is the biochemical oxygen demand (BOD) index, which is approached in different ways. In [12, 13], the authors propose a method based on biosensors and correlation calculations to obtain representative information on this indicator. This article presents another alternative approach that introduces an adaptive algorithm for river monitoring, extending the LookUp zonal algorithm approach published in [14], [15]. In addition to the challenges of estimating BOD in rivers, sudden weather anomalies also have an impact, introducing various sources of pollution that are difficult to identify. These sources tend to have adverse effects on aquatic ecosystems. To address monitoring issues in ecological systems, machine learning methods, time series analysis and statistical models are being used to make water management more objective, reliable and efficient [16–19]. In addition, some authors have integrated Bayesian networks with mechanistic models to fully exploit the advantages of statistical and mechanistic models in analyzing water quality risks during pollution emergencies. The results have been applied to various measurement indicators [20, 21]. The main problem in signal reconstruction for monitoring or control purposes is estimation, which involves reconstructing a useful signal while eliminating unwanted interference from another signal. This process aims

*e-mail: tadeusz.kwater@pwste.edu.pl

Manuscript submitted 2024-01-25, revised 2024-01-25, initially accepted for publication 2024-03-21, published in July 2024.

to preserve the quality of the signal containing important information by separating it from interference. Direct interference suppression techniques may inadvertently remove some of the useful signals. Therefore, optimal filters are used that take advantage of the statistical properties of the signals. One notable example is the Kalman filter, which recursively determines the state vector estimate with minimum variance in linear models of dynamic systems based on output measurements of the system [22–24]. It should be noted that the Kalman approach assumes linearity of the object model and knowledge of the characteristics of disturbances, which limits its application to idealized situations that do not fully reflect reality. The linearity requirement and assumptions about interference characteristics are limitations for the Kalman filter, since most systems are nonlinear and measurements are subject to non-Gaussian noise, such as Levy noise. These limitations are circumvented, among others, by using the approach proposed in this paper. The structure of this article is as follows: Section 2 gives the mathematical model and its transformation reducing the notation to a set of ordinary differential equations, Section 3 describes the new approach in the form of an adaptive zonal algorithm with a measurement window, the following section gives the experimental results including monitoring quality indicators, the final section summarizes the presented study.

2. MATHEMATICAL MODEL OF THE SPREAD OF POLLUTANTS IN THE RIVER

The issue of pollutant dispersion in a river is important for monitoring water quality. However, it is a very complex process that, when pollutants are discharged, generates processes that determine their spread and transport. Among these processes we have advection, diffusion, adsorption, desorption, settling of suspended substances, chemical reactions and biological processes [25]. The primary indicators characterizing the pollution status of a river include Biochemical Oxygen Demand (BOD) and Dissolved Oxygen Deficit (DO). These are the two indicators most commonly used to determine water quality and its ability to support aquatic life. The BOD index refers to the amount of oxygen required for microorganisms to oxidize organic matter in water under certain conditions. It is an indicator that measures the content of organic substances, such as carbon, nitrogen and phosphorus compounds, which can come from pollution, in a water sample. The higher the BOD, the greater the amount of organic matter present, which can lead to a shortage of oxygen in the water as microorganisms break it down. The DO deficit index reflects the amount of dissolved oxygen in the water compared to its full capacity. Dissolved oxygen deficit occurs when the concentration of oxygen in the water is lower than optimal for aquatic organisms. It can be caused by various factors, such as the presence of chemicals, organic pollutants or reduced water aeration. Low dissolved oxygen levels can lead to hypoxia in aquatic organisms and negatively affect aquatic ecosystems. A water body with very low DO levels is considered a dead body of water. Both BOD and DO are important water quality indicators that can be monitored to assess the extent of pollution and the health of aquatic ecosystems. High BOD values and low dissolved oxygen levels may indicate the presence of organic contaminants or other water quality problems that may require protective or corrective action. Monitoring these indicators can help identify potential risks and take appropriate action to protect and preserve water health. Further considerations will include a mathematical model describing these indicators to support the real-time monitoring process. In online monitoring issues, solutions are sought that bypass the complexity of calculations while maintaining the required accuracy of the solution. Due to the natural nature of the river, the determination of the dynamics of pollutant concentrations requires an indication of place and time. Thus, a model that determines the level of pollutant concentration in the form of partial differential equations is adopted. In the case of a mathematical model of a river, some simplifications can be made that cause a very slight loss of accuracy, due to the specifics of the object itself. The general mathematical model of a river, describing biochemical pollution and the process of self-purification takes the following form:

$$\frac{\partial x(l,t)}{\partial t} + v(l,t)\frac{\partial x(l,t)}{\partial l} = \mathbf{A}x(l,t) + w_R(l,t), \tag{1}$$

with initial (boundary) conditions:

$$IC: x(l,t_0) = x_0(l) + v_R(l), \tag{2}$$

$$BC: x(0,t) = x_B(t) + v_p(t), \tag{3}$$

where: $x(l,t)$ – vector $x(l,t) = \mathrm{col}[x_1(l,t), x_2(l,t)]$ with BOD and DO components expressed in [mg/l], $\mathbf{A} = \begin{bmatrix} k_1 & 0 \\ k_2 & k_3 \end{bmatrix}$ – coefficient matrix k_i, $i = 1,2,3$, $v_R(l)$, $v_p(t)$ – disturbances occurring in boundary conditions, $w_R(l,t)$ – disturbances interacting along the length of the river, x_1 – concentration of biochemical pollutants expressed in terms of BOD, x_2 – DO dissolved oxygen concentration deficit, which is the difference $x_2 = x_{2S} - x_{2N}$ between the dissolved oxygen concentration x_{2S} and the oxygen content of the water in the saturated state x_{2N}. The coefficients k_1, k_2 and k_3 appearing in the equations describe the dynamics of the river's natural self-purification process and depend primarily on temperature, in particular, they stand for: k_1 – reaction rate coefficient of BOD [1/day], k_2 – coefficient of the influence of BOD on DO [1/day], k_3 – coefficient of change of DO [1/day]. In the implementation of the monitoring task in real-time mode, it is sought, as far as possible, to reduce the complexity of calculations. Therefore, the authors for this purpose transform the mathematical model described by partial differential equations to a simpler form, i.e. ordinary differential equations, keeping the accuracy of the description unchanged. In particular, it is proposed to conduct considerations along the so-called characteristics. These characteristics will be lines defined by the flow velocity $v(l,t)$, and the description of the distribution of pollutant concentrations in the river refers to a freely moving volume of water (Fig. 1).

This interpretation of the model amounts to a transformation in which the observation of the distribution of pollution

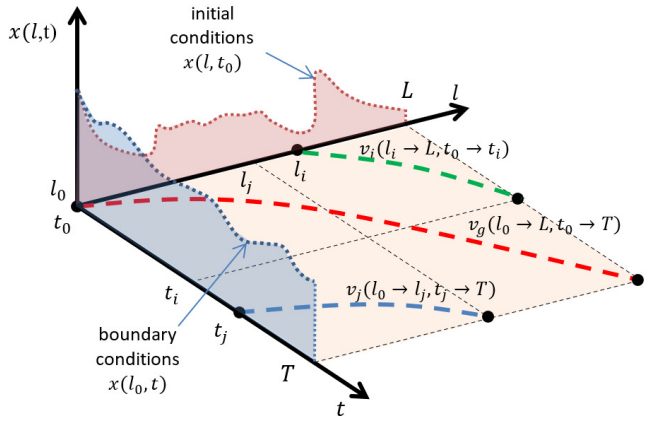

Fig. 1. The field of solutions using characteristics

in the river is made along the so-called characteristics in the spatio-temporal domain. To preserve the identity of the function describing the values of the state coordinates x in the spatio-temporal domain (the solution of hyperbolic partial differential equations), boundary conditions from the description of the model by differential equations with distributed parameters are used. The initial condition and the Dirichlet boundary condition are used for consideration (see Fig. 1) This means that the values of these functions are available for any length of the river and at any time in the area. River water pollution levels considered according to the characteristics in the l,t domain become ordinary differential equations representing the individual characteristics. The description of the vector x in the l,t domain leads to the solution of a number of spatio-temporal characteristics. As a result of this interpretation, for a known flow velocity v of the river, the distribution of pollution depends only on time, so, the characteristics are defined by the relation:

$$\frac{\mathrm{d}}{\mathrm{d}t}(l,t) = v(l(t)). \tag{4}$$

The characteristics shown in Fig. 1 describe the x vector in the following domain areas (l,t):

- i-th characteristic:

$$v_i(l(t)) = \left.\frac{\mathrm{d}}{\mathrm{d}t}(l,t)\right|_{t=t_0},$$
$$l(t) = \int_{t_0}^{t_i} v_i(t)\,\mathrm{d}t, \quad l(t) \in [l_i, L], \tag{5}$$

- main characteristic:

$$v_g(l(t)) = \left.\frac{\mathrm{d}}{\mathrm{d}t}(l,t)\right|_{t=t_0},$$
$$l(t) = \int_{t_0}^{T} v_g(t)\,\mathrm{d}t, \quad l(t) \in [l_0, L], \tag{6}$$

- j-th characteristic:

$$v_j(l(t)) = \left.\frac{\mathrm{d}}{\mathrm{d}t}(l,t)\right|_{t=t_j},$$
$$l(t) = \int_{t_j}^{T} v_j(t)\,\mathrm{d}t, \quad l(t) \in [l_0, l_j]. \tag{7}$$

This interpretation results in a set of characteristics covering the entire solution domain, and the equation for each characteristic takes the form of:

$$\frac{\mathrm{d}}{\mathrm{d}t}x(t) = \mathbf{A}x(t) + \mathbf{B}w(t), \tag{8}$$

where: x – state vector $x = \mathrm{col}[x_1, x_2]$, $\mathbf{A}$ – coefficient matrix as in equation (1), $\mathbf{B}$ – interaction matrix of interference signals, w – system disturbances vector $[w_1, w_2]$, w_1 – intensity of the inflow of pollutants [mg/l/day], w_2 – intensity of oxygen uptake/supply from/to water [mg/l/day].

Experimental studies use a set of equations (8) in the considered spatio-temporal domain, the number of which results from the density of these characteristics. It can be assumed that the discretization step on length l for a partial differential equation (1) is a parameter that determines the size of the set of ordinary differential equations (8).

The above assumptions make equation (8) a nonlinear ordinary differential equation, which will be used in further considerations. For the purposes of online monitoring, such measurements are chosen that can be made directly and without delay. For the issues under consideration, such a signal is $x_2(t)$. The general notation of the measurement equation takes the form:

$$y(t) = Cx + v_p, \tag{9}$$

where: $C = [01]$ – measurement matrix, v_p – measurement disturbances.

It should be noted that both the measurement and x signals are subject to noises with a Gaussian distribution [26].

3. ADAPTIVE ZONAL ALGORITHM WITH MEASUREMENT WINDOW

The proposed adaptive algorithm with a measurement window (LookUpWindow) generates all signals of the object, including those for which measurements are not made due to the difficulty of online measurement. The concept of the algorithm is to use a filtering equation with the structure as used in the Kalman filter. However, the gain value will be determined adaptively by incrementally modifying the gain ΔK. Specifically, the modification of the gain coefficient is carried out at each measurement step taking into account the current adaptation error ϵ_i, the history of measurements, and considering cases of their random absence. The adaptation error is a real, measurable signal, representing the difference between the current measurement $y(t)$ and the corresponding coordinate of the monitored signal vector $\widehat{x}$ and

was expressed by the equation:

$$\epsilon_i = y_i - C\widehat{x}_i\,, \tag{10}$$

where: ϵ_i – adaptation error in the i-th step. On the basis of the adaptive error ϵ_i equation (10), which is determined on the fly, an appropriate selection is made of the value of gain correction ΔK depending on the error's belonging to the designated error zones as illustrated in Fig. 2.

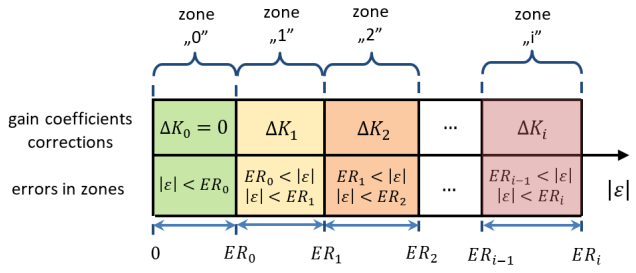

Fig. 2. Zones and their corresponding gain corrections ΔK_i in the correction table for zones

If the error value ϵ is less than the assumed error range ER_0 (zone "0"), then the gain factor correction is zero. This means that the actual monitoring error is at most equal to the permissible error range. Depending on the current adaptation error is selected gain factor correction from the adopted correction table for zones. In special cases of missing measurements, the gain update is skipped.

It is worth noting that the gain is updated using corrections derived from the value of the adaptation error, and an adjustment is made to take into account several previous measurements. This is due to the use of a measurement window in the algorithm, which includes the history of measurements. Figure 3 shows a diagram of the moving measurement window D and the weight distributions of the measurements. The presented moving measurement window D includes q measurements. which means that the history of measurements is taken into account. However, the adopted distribution of weights for individual measurements causes that we get the effect of "aging" of measurements as the window moves. This means that a measurement that was current previously is now treated as "obsolete". Assigning smaller

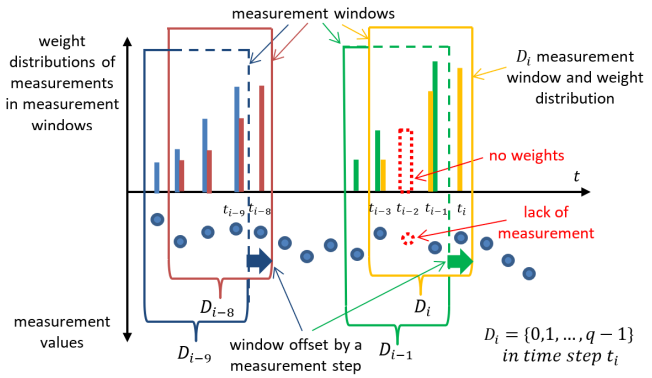

Fig. 3. Variability of the distribution of measurement weight values in a moving measurement window

and smaller weights corresponds to increasingly older measurements in the measurement window (see Fig. 3). If there is no measurement, the distribution of weights in the window is modified, which means that the remaining weights of measurements in the window are increased accordingly. The measurement window D_i includes the measurement at the current step t_i and the measurements from previous steps t_{i-1}, and t_{i-3}, and as a result of the absence of a measurement at time t_{i-2}, the weight for that measurement is zero.

According to the assumptions for determining gain values, an update is made to the current gain resulting from the adaptation error (see Fig. 2) according to the relation:

$$Ks_{i+1} = Ks_i + \Delta K_j\,, \tag{11}$$

where: Ks_i – current value of gain, ΔK_j – gain correction for the j-th zone from the adopted zone table. Then, the correction forcing of the estimate M_{i+1} resulting from the measurement window for the next measurement step is determined according to the equation:

$$M_{i+1} = \sum_{j=0}^{q} w_j Ks_{i-j}\left(y_{i-j} - C\widehat{x}_{i-j}\right). \tag{12}$$

Ks_{i-j} – gain in the measurement window from the current Ks_i to the last in the window Ks_{i-q}, w_j – measurement weights from w_0 to w_q, q – quantity of measurements in the measurement window.

In the next iteration, the correction forcing of the estimate takes the index i, and the equation that generates the object signals in the monitoring system takes the form of:

$$\widehat{x}_i = \mathbf{A}\widehat{x}_i + M_i \tag{13}$$

M_i – correction forcing of the estimate.

A detailed description of the algorithm for monitoring an object with randomly missing measurements is presented in pseudo-code form in Algorithm 1.

In cases of obtaining information from the object in the form of measurements, Algorithm 1 updates the filter gain coefficient Ks_i by the adopted gain correction ΔK_j depending on the affiliation of the current adaptation error ϵ_i to the zone defined by the value of the error range ER_i (lines 9 and 12). Then, the correction forcing of the estimate resulting from the application of the measurement window is determined (line 15). If the value of the adaptation error ϵ is less than the error limit ER_0, then the gain update resulting from the adaptation error is not performed (line 6). Calculation of the correction forcing of the estimate derived from the measurement window is performed in each iteration. The algorithm can be easily extended to additional zones, which can be implemented in line 14.

3.1. Measures of the quality of monitoring

Two indicators, i.e. Root Mean Squared Error (RMSE) and Mean Absolute Error (MAE), were adopted to measure the quality of online monitoring of the time courses of BOD and DO signals using the presented algorithm.

Algorithm 1 Adaptive zonal algorithm with measurement window (LookUpWindow)

$\widehat{x}_0, Ks_0, M, \Delta K, ER, q$, *distribution of weights* $(w_0, \ldots, w_q)$, i, n, A // setting the initial conditions
Input: y_i //measurements
Output: $\widehat{x}$

while $i < n$ **do**
  $\widehat{\dot{x}}_i \leftarrow \mathbf{A}\widehat{x}_i + M_i$ // determination of the estimate
  if *mesurement* **then**
    $\epsilon_i \leftarrow y_i - C\widehat{x}_i$;
    if $\epsilon_i \le ER_0$ **then**
      $Ks_{i+1} \leftarrow Ks_i$;
    end if
    if $ER_0 < \epsilon_i \le ER_1$ **then**
      $Ks_{i+1} \leftarrow Ks_i + \Delta K_1$;
      // ΔK selection and gain updating
    end if
    if $ER_1 < \epsilon_i \le ER_2$ **then**
      $Ks_{i+1} \leftarrow Ks_i + \Delta K_2$;
      // ΔK selection and gain updating
    end if
    . . . more zones
    $M_{i+1} \leftarrow \sum_{j=0}^{q} w_j Ks_{i-j}(y_{i-j} - C\widehat{x}_{i-j})$;
    // calculation of the correction forcing of the estimate from the D_i window
  else
    modifying the distribution of weights in the D_i *window with missing measurements*;
    $M_{i+1} \leftarrow \sum_{j=0}^{q} w_j Ks_{i-j}(y_{i-j} - C\widehat{x}_{i-j})$;
    // calculation of the correction forcing of the estimate from the D_i window
  end if
  $i \leftarrow i+1$;
end while

The first indicator is a mean-square error and has a high sensitivity to estimation deviations from actual values. The value of the RMSE indicator is more influenced by large errors. In addition, RMSE always takes a positive value and is expressed in units of forecast signals [27].

For the investigated signals, the value of the RMSE index is determined according to the formula:

$$RMSE_i = \sqrt{\frac{1}{n}\sum_{j=1}^{n} e_{i,j}^2}, \tag{14}$$

where: i – index of monitored signal, $e_{i,j} = x_{i,j} - \widehat{x}_{i,j}$ – estimation error of the i-th signal in the j-th step, n – number of simulation steps. The second indicator is the mean absolute estimation error of the MAE determined according to the relationship:

$$MAE_i = \frac{1}{n}\sum_{j=1}^{n} \left| e_{i,j} \right|. \tag{15}$$

MAE is easier to interpret its value. In addition, it is less sensitive to large errors, which have little effect on the MAE value [24].

4. RESULTS OF SIMULATION STUDIES

Simulation experiments were conducted for a hypothetical river described by ordinary differential equations, according to the so-called characteristics. A river flowing at an average velocity of $v = 30$ [km/day] with two large polluted tributaries and an area of several tens of kilometers with an intense inflow of pollutants were considered.

The simulation studies presented here cover signals obtained from the assumed mathematical model and signals generated using adaptive algorithms: zonal LookUp_z [15] and the proposed zonal with measurement window LookUp_w, as well as the Kalman filter. The results also include cases of random missing measurements with different frequencies of occurrence.

Figure 4 shows the waveforms of BOD and DO signals on the selected characteristic over a 36-day period, where the influence of lateral inflows is evident in the form of large BOD values at the beginning of the simulation period and on day 24. A sudden increase in BOD also occurs on day 12 and continues for several days. The interpretation of such a situation relates to intensive inflows of pollutants caused by large rainfalls lasting in the area of the river's course. It should be emphasized that such a character of changes in the forcing of BOD concentrations makes large, even quite unnatural, demands on the estimated signals. The unmeasured BOD signals obtained with different algorithms take on positive values. The negative signals relate to the DO deficit, the measurement of which is easy to implement, hence the high similarity of the obtained waveforms. The measurement window and zonal algorithms (red and black, respectively) generate signals of comparable quality, i.e., the generated signals are close to the model values, while the signals from the Kalman filter (green) show greater discrepancies.

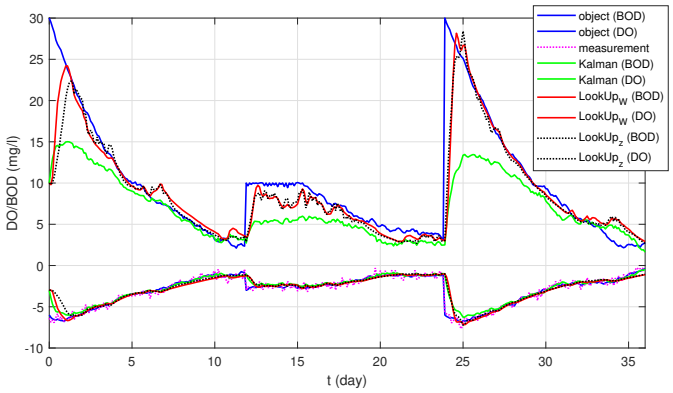

Fig. 4. BOD and DO signals obtained with LookUpWindow, LookUp and Kalman filter algorithms

The resulting BOD and DO signals in Fig. 4 result from different values of the gains generated by the algorithms, and their waveforms are presented in Fig. 5. The highest values of amplifications appear after sudden large changes in the forcing, which means the natural response of the algorithm, to the occurrence

of large errors. A characteristic feature of the considered cases is the amplifications of different signs and amplitudes for BOD and DO signals.

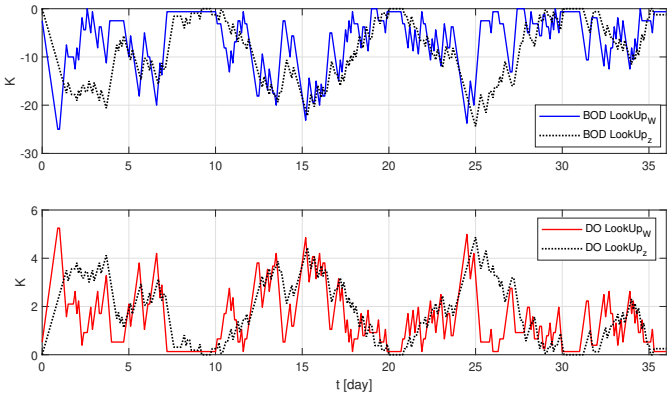

Fig. 5. Gain coefficients generated by LookUpWindow and LookUp algorithm

The study includes cases of random lack of delivery of measurements. In practice, such a situation can refer to the failure of the measurement system caused, for example, by temporary shortages of power supply or transmission of signals.

Figure 6 shows measurement moments with missing measurements as points on the time axis. Despite the random absence of 20% of measurements, the algorithms generated waveforms of similar quality (compare with Fig. 4). The experiments extend the cases where missing measurements amounted to several tens of percent (see Table 1) Despite the large lack of measurements (69%), the algorithms do not lose stability of performance. To illustrate the correctness of the algorithms for difficult situations caused by the absence of a large number of measurements, selected waveforms of generated signals and gains are shown in Fig. 7 and Fig. 8. The zone algorithm, in the absence of a large number of measurements, showed a larger amplitude of change in gain coefficients compared to the algorithm with a measurement window. Despite this behaviour, the quality of signals generated by the algorithm with the measurement window is much better compared to the other algorithms. The quality of the results obtained in the algorithm with a measurement window also depends on the assumed distribution of measure-

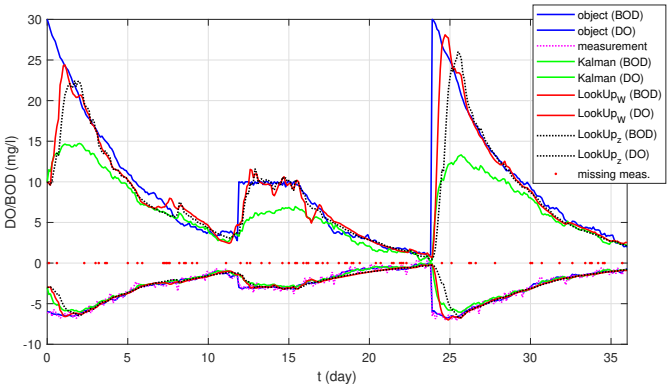

Fig. 6. BOD and DO signals obtained with the tested algorithms at random lack of 20% of measurements

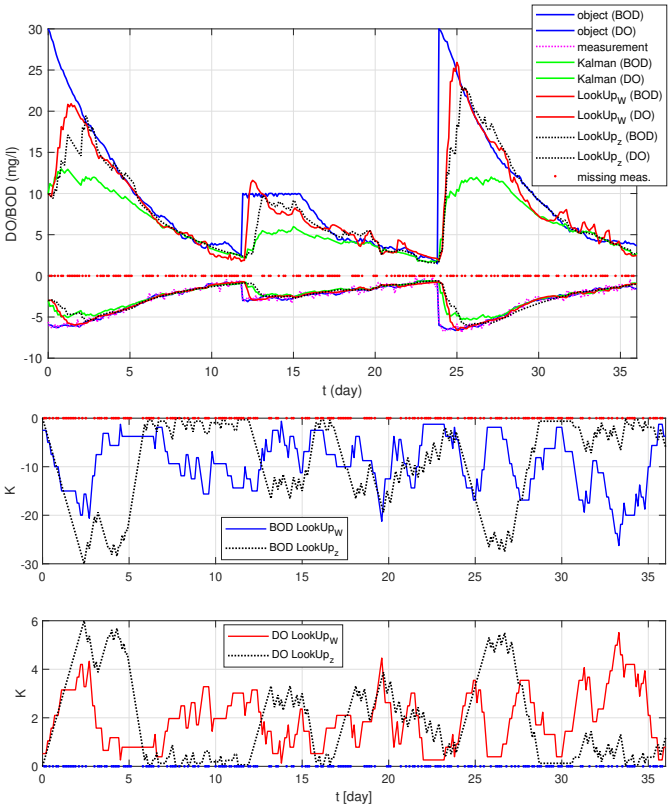

Fig. 7. BOD and DO signals and gains generated by the tested algorithms at a random lack of 185 out of 360 possible measurements

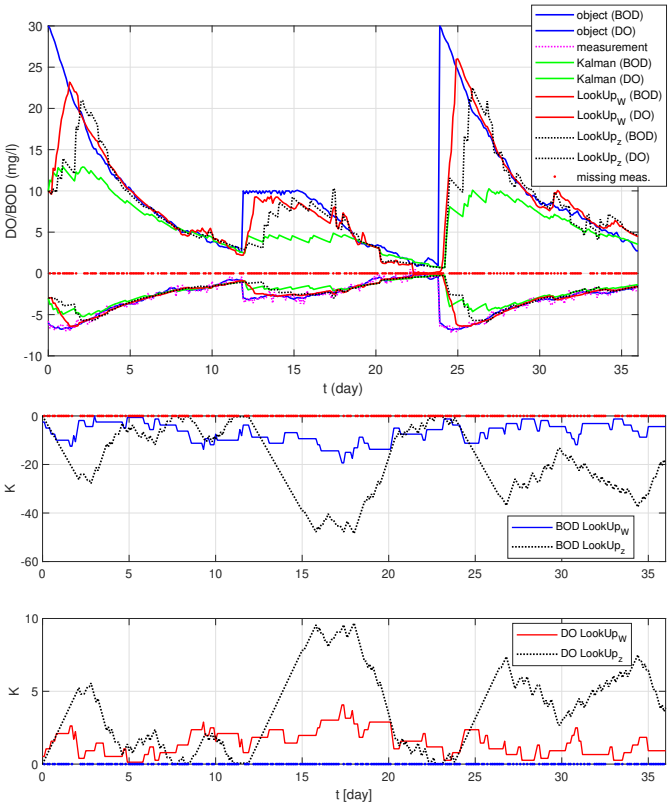

Fig. 8. BOD and DO signals and gains generated by the tested algorithms at a random lack of 262 out of 360 possible measurements

Table 1
Monitoring quality of BOD and DO signals for different numbers of randomly missing measurements

LookUpWindow	RMSE		MAE	
estimated signal	BOD	DO	BOD	DO
all 360 measurements	3.765	0.598	1.850	0.272
20% (lack of 71)	3.553	0.629	1.848	0.275
49% (lack of 176)	3.722	0.695	1.879	0.326
69% (lack of 250)	3.986	0.649	2.102	0.314
$LookUp_z$	RMSE		MAE	
estimated signal	BOD	DO	BOD	DO
all 360 measurements	3.697	0.697	1.904	0.323
20% (lack of 71)	4.139	0.805	1.972	0.357
49% (lack of 176)	4.284	0.833	2.147	0.395
69% (lack of 250)	4.718	0.996	2.392	0.505
Kalman filter	RMSE		MAE	
estimated signal	BOD	DO	BOD	DO
all 360 measurements	5.293	0.604	3.110	0.306
20% (lack of 71)	5.520	0.707	3.227	0.360
49% (lack of 176)	5.972	0.898	3.562	0.492
69% (lack of 250)	6.139	0.958	3.794	0.595

ment weights. Table 2 shows the values of the RMSE and MAE quality indicators for different distributions of the measurement window weights. Increasing the values of the weights slightly improves the quality of the estimation assessed by the RMSE index, but in the case of the MAE index, a deterioration in quality can be observed with larger values of the measurement weights.

Table 2
Monitoring quality of BOD and DO signals for different distributions of the measurement window weights

RMSE	LookUpWindow		$LookUp_z$		Kalman filter	
estimated signal	BOD	DO	BOD	DO	BOD	DO
0.6; 0.35; 0.15; 0.05	3.488	0.662				
1.2; 0.7; 0.3 ;0.1	3.189	0.577	4.21	0.88	5.20	0.62
2.4; 1.4; 0.6; 0.2	3.110	0.564				
MAE	LookUpWindow		$LookUp_z$		Kalman filter	
estimated signal	BOD	DO	BOD	DO	BOD	DO
0.6; 0.35; 0.15; 0.05	1.407	0.297				
1.2; 0.7; 0.3; 0.1	1.419	0.271	1.75	0.41	3.00	0.34
2.4; 1.4; 0.6; 0.2	1.647	0.302				

5. CONCLUSIONS

This paper presents an adaptive algorithm that generates online object signals based on online measured state coordinates. A mathematical model of a river described by ordinary differential equations, for which water quality is represented by BOD and DO deficit indicators, was used as a test object.

The algorithm estimates the BOD signal based on the DO signal measurements made online. During the estimation of signals in the algorithm, adaptive changes are made to the gain coefficients using an incremental method. The correction values are determined for the zones in the array, and also result from updating the weights in the measurement window. The proposed algorithm does not require knowledge of the characteristics of the enforcing signals that interact with the object and measurements. The algorithm is in the form of additive filter gain correction, and it uses a predefined adaptive error and a history of measurements that takes into account their weights. In addition, the approach takes into account random lack of measurements, which did not much deteriorate the quality of the estimation. In all cases studied, the zonal algorithm with a measurement window provided better estimation results, as measured by the RMSE and MPE quality indicators, than the zonal algorithm without a measurement window and Kalman filter. This was particularly evident for the estimation of the unmeasured state coordinate, BOD.

The presented concept of a zonal algorithm with a measurement window applied to monitoring an object described by a mathematical model representing only two water quality indicators, i.e. BOD and DO, works well. Satisfactory results should also be expected with further expansion of the mathematical model to include other water quality indicators.

REFERENCES

[1] P.M. Pujar, H.H. Kenchannavar, R.M. Kulkarni, and U.P. Kulkarni, "Real-time water quality monitoring through internet of things and anova-based analysis: a case study on river krishna," *Appl. Water Sci.*, vol. 10, p. 22, 2020, doi: 10.1007/s13201-019-1111-9.

[2] M.S.U. Chowdury, T.B. Emran, S. Ghosh, A. Pathak, M.M. Alam, N. Absar, K. Andersson, and M.S. Hossain, "Iot based real-time river water quality monitoring system," *Procedia Comput. Sci.*, vol. 155, pp. 161–168, 2019, doi: 10.1016/j.procs.2019.08.025.

[3] R. Bogdan, C. Paliuc, M. Crisan-Vida, S. Nimara, and D. Barmayoun, "Low-cost internet-of-things water-quality monitoring system for rural areas," *Sensors*, vol. 23, p. 3919, 4 2023. [Online]. Available: https://wScienceoftheTotalEnvironmentww.mdpi.com/1424-8220/23/8/3919

[4] Q. Cao, G. Yu, S. Sun, Y. Dou, H. Li, and Z. Qiao, "Monitoring water quality of the haihe river based on ground-based hyperspectral remote sensing," *Water*, vol. 14, pp. 1–13, 2022.

[5] P. Jayaraman, K.K. Nagarajan, P. Partheeban, and V. Krishnamurthy, "Critical review on water quality analysis using iot and machine learning models," *Int. J. Inf. Manage. Data Insights*, vol. 4, no. 1, p. 100210, 2024. [Online]. Available: https://www.sciencedirect.com/science/article/pii/S2667096823000563

[6] A.M. Meyer, C. Klein, E. Fünfrocken, R. Kautenburger, and H.P. Beck, "Real-time monitoring of water quality to identify pollution pathways in small and middle scale rivers," *Sci. Total Environ.*, vol. 651, pp. 2323–2333, 2 2019. [Online]. Available: https://linkinghub.elsevier.com/retrieve/pii/S0048969718339421

[7] R. Sulistyowati, A. Suryowinoto, A. Fahruzi, and M. Faisal, "Prototype of the monitoring system and prevention of river water pollution based on android," *IOP Conference Series: Materials Science and Engineering*, vol. 462, p. 012028, 1 2019. [Online]. Available: http://stacks.iop.org/1757-899X/462/i=1/a=012028?key=crossref.12c7f68b5ec586bb105187aa95489053

[8] T. Shu, M. Xia, J. Chen, and C.D. Silva, "An energy efficient adaptive sampling algorithm in a sensor network for automated water quality monitoring," *Sensors*, vol. 17, p. 2551, 11 2017.

[9] I. Yaroshenko, D. Kirsanov, M. Marjanovic, P.A. Lieberzeit, O. Korostynska, A. Mason, I. Frau, and A. Legin, "Real-time water quality monitoring with chemical sensors," *Sensors*, vol. 20, pp. 1–22, 6 2020.

[10] O. Kanoun, T. Lazarević-Pašti, I. Pašti, S. Nasraoui, M. Talbi, A. Brahem, A. Adiraju, E. Sheremet, R.D. Rodriguez, M.B. Ali, and A. Al-Hamry, "A review of nanocomposite-modified electrochemical sensors for water quality monitoring," *Sensors*, vol. 21, p. 4131, 6 2021. [Online]. Available: https://www.mdpi.com/1424-8220/21/12/4131

[11] D. Sun, B. Xie, J. Li, X. Huang, J. Chen, and F. Zhang, "A low-cost microbial fuel cell based sensor for in-situ monitoring of dissolved oxygen for over half a year," *Biosens. Bioelectron.*, vol. 220, p. 114888, 2023. [Online]. Available: https://www.sciencedirect.com/science/article/pii/S0956566322009289

[12] P. Villalobos, C.A. Acevedo, F. Albornoz, E. Sánchez, E. Valdés, R. Galindo, and M.E. Young, "A bod monitoring disposable reactor with alginate-entrapped bacteria," *Bioprocess Biosyst. Eng.*, vol. 33, pp. 961–970, 10 2010.

[13] H. Lin, N. Xu, G. Xing, Y. Shang, X. Wang, and L. Lin, "Microfluidic chip-based microbial metabolism-indexed bod sensor for rapid determination of biochemical oxygen demand," *Sens. Actuator B-Chem.*, vol. 400, p. 134868, 2024. [Online]. Available: https://www.sciencedirect.com/science/article/pii/S0925400523015861

[14] P. Hawro, T. Kwater, and D. Strzęciwilk, "The monitoring system based on lookup algorithm for objects described by ordinary differential equations," *ITM Web Conf.s*, vol. 21, p. 00006, 10 2018. [Online]. Available: https://www.itm-conferences.org/10.1051/itmconf/20182100006

[15] P. Hawro, T. Kwater, J. Bartman, and B. Kwiatkowski, "The look-up algorithm of monitoring an object described by nonlinear ordinary differential equations," *Bull. Pol. Acad. Sci. Tech. Sci.*, vol. 71, no. 2, p. e144603, 2023.

[16] A.N. Ahmed, F.B. Othman, H.A. Afan, R.K. Ibrahim, C.M. Fai, M.S. Hossain, M. Ehteram, and A. Elshafie, "Machine learning methods for better water quality prediction," *J. Hydrol.*, vol. 578, no. 11, p. 124084, 2019, [Online]. Available: https://linkinghub.elsevier.com/retrieve/pii/S0022169419308194

[17] Z. Di, M. Chang, and P. Guo, "Water quality evaluation of the yangtze river in china using machine learning techniques and data monitoring on different time scales," *Water*, vol. 11, no. 2, p. 339, 2019.

[18] L.F. Arias-Rodriguez, Z. Duan, J. de Jesús Díaz-Torres, M.B. Hazas, J. Huang, B.U. Kumar, Y. Tuo, and M. Disse, "Integration of remote sensing and mexican water quality monitoring system using an extreme learning machine," *Sensors*, vol. 21, no. 6, p. 4118, 2021. [Online]. Available: https://www.mdpi.com/1424-8220/21/12/4118

[19] J. Geng, C. Yang, Y. Li, L. Lan, and Q. Luo, "Mpa-rnn: A novel attention-based recurrent neural networks for total nitrogen prediction," *IEEE Trans. Ind. Inform.*, vol. 18, no. 10, pp. 6516–6525, 2022. [Online]. Available: https://ieeexplore.ieee.org/document/9741344/

[20] E. Bertone, O. Sahin, R. Richards, and R.A. Roiko, "Bayesian network and system thinking modelling to manage water-related health risks from extreme events," in *2015 IEEE International Conference on Industrial Engineering and Engineering Management (IEEM)*. IEEE, 12 2015, pp. 1272–1276. [Online]. Available: http://ieeexplore.ieee.org/document/7385852/

[21] C. Tang, Y. Yi, Z. Yang, and J. Sun, "Risk forecasting of pollution accidents based on an integrated bayesian network and water quality model for the south to north water transfer project," *Ecol. Eng.*, vol. 96, nno. 11, pp. 109–116, 2016. [Online]. Available: https://linkinghub.elsevier.com/retrieve/pii/S0925857415302809

[22] C. Wellen, G.B. Arhonditsis, T. Long, and D. Boyd, "Accommodating environmental thresholds and extreme events in hydrological models: A bayesian approach," *J. Great Lakes Res.*, vol. 40, pp. 102–116, 2014. [Online]. Available: https://linkinghub.elsevier.com/retrieve/pii/S0380133014000744

[23] G. Feng, C. Lai, and N.C. Kar, "Expectation maximization particle filter and Kalman filter based permanent magnet temperature estimation for PMSM condition monitoring using high-frequency signal injection," *IEEE Trans. Ind. Inform.*, vol. 13, no. 3, pp. 1261–1270, 2017. [Online]. Available: http://ieeexplore.ieee.org/document/7513373/

[24] J.-M. Guihal, F. Auger, N. Bernard, and E. Schaeffer, "Efficient implementation of continuous-discrete extended kalman filters for state and parameter estimation of nonlinear dynamic systems," *IEEE Trans. Ind. Inform.*, vol. 18, no. 5, pp. 3077–3085, 2022. [Online]. Available: https://ieeexplore.ieee.org/document/9527070/

[25] E.R. Holley, "Field tests for evaluating hydraulic transport process in rivers," *Publications of the Institute of Geophysics Polish Academy of Sciences*, vol. E-2(325), pp. 39–51, 2001.

[26] R. Ranojidoss, V.P. Sandhya, and V. Vamsikrishnamuvalla, "State estimation of concentration in cstr by extended kalman filter," *Int. J. Adv. Res. Electr. Electron. Instrum. Eng.*, vol. 3, pp. 152–156, 2014.

[27] T. Chai and R.R. Draxler, "Root mean square error (rmse) or mean absolute error (mae)? – arguments against avoiding rmse in the literature," *Geosci. Model Dev.*, vol. 7, pp. 1247–1250, 2014.